International Journal of Electrical and Power Engineering 2 (6): 415-424, 2008
ISSN: 1990-7958

The Enhancement of Dynamic Performance of Cascaded Induction Motors Using SVC and D-STATCOM

Pirooz Javanbakht and Mehrdad Abedi
Amirkabir University of Technology (Tehran Polytechnic), Hafez Avenue, Tehran, Iran

Abstract: This study presents the comparative studies in order to evaluate the effects of Static Var Compensator (SVC) and Distribution Static Synchronous Compensator (D-STATCOM) on dynamic and transient performance of Common Shaft Cascaded Induction Motors (CSCIMs) which are commonly used in deep well digging plant (i.e. oil wells). The dynamic and transient events presented in this paper include system starting, supply voltage sag and swell as well as supply disconnection and reconnection. Modeling and simulation results of the presented events are based on well known MATLAB/ Sim Power Systems (SPS) blocks. The simulation results show that the D-STATCOM has a superior performance over SVC.

Key words: Common shaft cascaded induction motor (CSCIM), Distribution static synchronous compensator (D-STATCOM), Flexible alternating current transmission system (FACTS), SimPowerSystems (SPS) blocks, Static var compensator

INTRODUCTION

The investigation of dynamic and transient behaviour of three phase induction motors has been an attractive subject (Kraus, 1965; Smith and Sriharam, 1967; Sarka and Berg, 1970; Nath and Berg, 1981; Lin *et al*., 1986) for a long time owing to their practical application in industry. For prediction of transient phenomena, appropriate modeling of induction machines is very important. Several models have been well developed such as phase coordinate and d, q models, which have even appeared in classical textbooks (Adkins and Harely, 1975; Krause, 1986; Boldea and Naser, 1986; Hancook, 1974).

The Static Var Compensator (SVC) is a shunt device in the Flexible Alternating Current Transmission Systems (FACTS) family using power electronic devices to enhance power system operation (Chang and Yu, 1999; Abdel-Rahman *et al*., 20069; Jing Zhang *et al*., 2007). The SVC can also be employed to enhance distribution system and industrial plant operation (Rastegar *et al*., 1999; Abedi *et al*., 1998). The SVC generally regulates voltage at its terminal by controlling the reactive power injected to or absorbed from the power network. In fact, the SVC generates or absorbs the reactive power when the terminal voltage is low and high, respectively. The variation of reactive power is performed by switching three phase capacitor or inductor banks. The SVC is usually composed of two main parts, namely:

- Thyristor Switched Capacitor (TSC).
- Thyristor Controlled Reactor (TCR).

The static synchronous compensator (STATCOM) is also a shunt device in FACTS family using power electronic devices to control power flow in order to enhance power network operation (Giroux *et al*., 2001; Freitas *et al*., 2005; Eldery *et al*., 2007; Sensarma *et al*., 2002). The STATCOM regulates its terminal voltage by controlling the reactive power injected to or absorbed from the system. The STATCOM performs the same function as the SVC, however, at the voltages lower than the normal voltage regulation range the STATCOM can generate more reactive power than the SVC. In addition, the STATCOM normally exhibits a faster response compared to SVC, due to its voltage source converter (VSC) in which provides no delay associated with thyristor firing (Sim Power Systems, 2006). In distribution network, STATCOM is called D-STATCOM which enhances the distribution network operation.

In the literature, little attention has been paid to evaluation of dynamic and transient performance of common shaft cascaded induction motors (CSCIMs), which are widely used in deep well digging schemes, particularly in the oil industry. In Ogata (1970) evaluation of transient performance of CSCIMs is reported. However, the effects of presently popular FACTS devices such as SVC and D-STATCOM on dynamic and transient

Corresponding Author: Pirooz Javanbakht, Amirkabir University of Technology (Tehran Polytechnic), Hafez Avenue, Tehran, Iran

behaviour of CSCIMs have not seen yet which in fact our main goal in this study is. In this study 3 dynamic and transient events are simulated using well known SPS (Sim Power Systems, 2006) library and the results are presented namely:

- System starting.
- Supply voltage sag and swell.
- Supply disconnection and reconnection.

SAMPLE SYSTEM

Figure 1 shows the general schematic diagram of the studied system which consists of n similar CSCIMs. The 3 phase stator windings are connected to 3 phase main bus (i.e. bus M). Bus M is also supplied by 20/2.3 kV, 15 MVA,Δ-Y 3 phase transformer (T1) and is connected to 3 phase feeder via Circuit Breaker (CB1). T1 is also fed by 2 km, 20 kV 3 phase distribution line connected to equivalent 20 kV, 500 MVA source. In the sample system we also provide the facility in order to connect SVC or D-STATCOM through 23 phase coupling transformers (T2 and T3) via 2 circuit breakers (CB2 and CB3) for further investigations.

Figure 1 also depicts the mass and spring configuration of all rotors in CSCIM scheme and illustrates the mechanical load and shaft stiffness due to different shaft segments. To represent the shaft inertia, two possible methods can be employed:

- One can assume that the whole shaft inertia (J_{sh}) is located at the end point of the common shaft (Fig. 1),
- One can assume that half of the inertia for each shaft segment is added to the rotor inertia of adjacent motors.

In this study, the first assumption has been employed.

PROBLEM FORMULATION FOR CSCIMS

Electrical model for the induction motor: In this study, the stationary d, q frame of reference has been employed for the induction motor modeling (Lin *et al*., 1986; Krause, 1986; Hancook, 1974). Stator windings are represented by two coils, each located on the d and q axes. The rotor windings are also modeled by 2 short circuited coils, one located on each axis. The electrical model for prediction of the transient performance of the jth motor in Fig. 1, based on the stationary d, q frame of reference is (Lin *et al*., 1986; Adkins and Harely, 1975; Krause, 1986; Boldea and Naser, 1986; Hancook, 1974):

$$pI_j = A_j I_j + B_j V_j \quad (1)$$

Where,

$$I_j = [i_{dsj} \quad i_{qsj} \quad i_{drj} \quad i_{qrj}]^T \quad (2a)$$

$$V_j = [V_{dsj} \quad V_{qsj} \quad V_{drj} \quad V_{qrj}]^T \quad (2b)$$

$$A_j = \frac{1}{\Delta_j}\begin{bmatrix} A_{11,j} & A_{12,j} \\ A_{21,j} & A_{22,j} \end{bmatrix} \quad (3a)$$

$$B_j = \frac{1}{\Delta_j}\begin{bmatrix} B_{11,j} & B_{12,j} \\ B_{21,j} & B_{22,j} \end{bmatrix} \quad (3b)$$

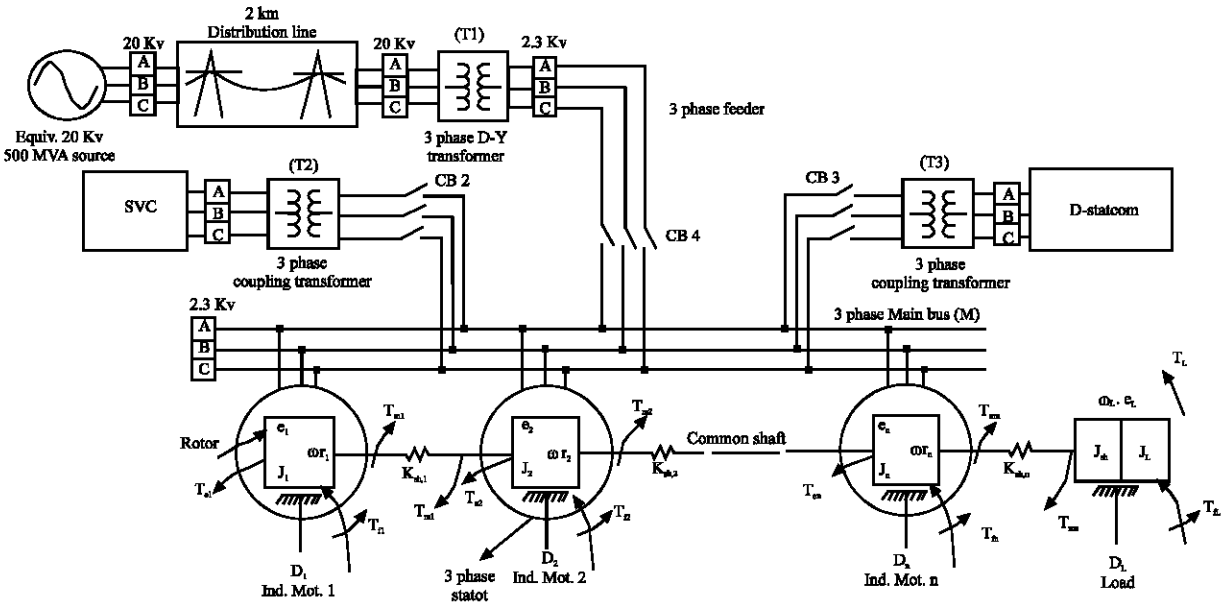

Fig. 1: Schematic diagram of the studied system

And:

$$A_{11,j}=\begin{bmatrix}-L_{rj}R_{sj} & M_j^2\omega_{rj}\\ -M_j^2\omega_{rj} & -L_{rj}R_{sj}\end{bmatrix} \quad (4a)$$

$$A_{12,j}=\begin{bmatrix}M_jR_{rj} & M_jL_{rj}\omega_{rj}\\ -M_jL_{rj}\omega_{rj} & M_jR_{rj}\end{bmatrix} \quad (4b)$$

$$A_{21,j}=\begin{bmatrix}M_jR_{sj} & -M_jL_{sj}\omega_{rj}\\ M_jL_{sj}\omega_{rj} & M_jR_{sj}\end{bmatrix} \quad (4c)$$

$$A_{22,j}=\begin{bmatrix}-L_{sj}R_{rj} & -L_{sj}L_{rj}\omega_{rj}\\ L_{sj}L_{rj}\omega_{rj} & -L_{sj}R_{rj}\end{bmatrix} \quad (4d)$$

$$B_{11,j}=L_{rj}I_2 \quad (5a)$$

$$B_{12,j}=B_{21,j}=-M_jI_2 \quad (5b)$$

$$B_{22,j}=L_{sj}I_2 \quad (5c)$$

$$\Delta_j=L_{rj}L_{sj}-M_j^2 \quad (6)$$

$$I_2=2\times2 \text{ unit matrix} \quad (7)$$

Note that:

$$L_{rj}=L_{lrj}+M_j \quad (8a)$$

$$L_{sj}=L_{lsj}+M_j \quad (8b)$$

The d, q components of the stator voltages for the jth motor in the stationary frame of reference are (Hancook, 1974):

$$V_{dqo,sj}=\sqrt{\frac{2}{3}}\,CV_{abc,sj} \quad (9)$$

Where,

$$V_{dqo,sj}=[V_{dsj}\quad V_{qsj}\quad V_{osj}]^T \quad (10a)$$

$$V_{abc,sj}=[V_{asj}\quad V_{bsj}\quad V_{csj}]^T \quad (10b)$$

$$C=\begin{bmatrix}1 & -\frac{1}{2} & -\frac{1}{2}\\ 0 & \frac{\sqrt{3}}{2} & -\frac{\sqrt{3}}{2}\\ \frac{1}{\sqrt{2}} & \frac{1}{\sqrt{2}} & \frac{1}{\sqrt{2}}\end{bmatrix} \quad (11)$$

But:

$$V_{abc,sj}=V_{mj}[\cos\lambda \quad \cos(\lambda-2\Pi/3)\ \cos(\lambda+2\Pi/3)]^T \quad (12)$$

Where,

$$\lambda=\omega_0t+\alpha$$

Thus:

$$V_{dqo,sj}=\sqrt{\frac{3}{2}}\,V_{mj}\,[\cos\lambda\ -\sin\lambda\ 0]^T \quad (13)$$

Since, the rotor windings are short circuited, it is clear that:

$$V_{dqo,rj}=[0\quad 0\quad 0]^T \quad (14)$$

The developed electromagnetic torque of the jth motor is:

$$T_{ej}=\frac{MjP}{2}\,(i_{drj}\ i_{qsj}-i_{qrj}\ i_{dsj}) \quad (15)$$

Mechanical dynamic equations: According to, Fig. 1, the equations of motion for each induction motor concerning the shaft torsion torque (i.e. shaft stiffness torque) in each shaft segment and the friction torque are:

$$J_1p\omega_{r1}=T_{e1}-T_{m1}-T_{f1} \quad (16a)$$

$$J_2p\omega_{r2}=T_{e2}+T_{m1}-T_{m2}-T_{f2} \quad (16b)$$

$$\vdots$$

$$J_jp\omega_{rj}=T_{ej}+T_{mj-1}-T_{mj}-T_{fj} \quad (16j)$$

$$\vdots$$

$$J_np\omega_{rn}=T_{en}+T_{mn-1}-T_{mn}-T_{fn} \quad (16n)$$

$$(J_L+J_{sh})\,p\omega_L=T_{mn}-T_L-T_{fL} \quad (16n+1)$$

It is assumed that (Ogata, 1970):

- The frictional torque is proportional to the speed.
- The torsion torque (i.e. stiffness torque) is proportional to the difference between the angular positions of both ends in each shaft segment. The constant of proportionality is called the stiffness factor. Thus:

$$J_1p\omega_{r1}=T_{e1}-k_{sh,1}(\theta_1-\theta_2)-D_1\,\omega_{r1} \quad (17a)$$

$$J_2p\omega_{r2}=T_{e2}+k_{sh,1}(\theta_1-\theta_2)-k_{sh,2}(\theta_2-\theta_3)-D_2\,\omega_{r2} \quad (17b)$$

$$\vdots$$

$$J_jp\omega_{rj}=T_{ej}+k_{sh,j-1}(\theta_{j-1}-\theta_j)-k_{sh,j}(\theta_j-\theta_{j+1})-D_j\,\omega_{rj} \quad 17j)$$

$$\vdots$$

$$J_np\omega_{rn}=T_{en}+k_{sh,n-1}(\theta_{n-1}-\theta_n)-k_{sh,n}(\theta_n-\theta_{n+1})-D_n\,\omega_{rn} \quad (17n)$$

$$(J_L+J_{sh})\,p\omega_L = k_{sh,n}(\theta_n - \theta_L) - T_L - D_L\,\omega_L \quad (17n+1)$$

Also:

$$p\theta_i = \omega_{ri} \quad I = 1, 2, \ldots, n \quad (18a)$$

$$p\theta_L = \omega_L \quad (18b)$$

General formulation: For complete system transient studies, the following electrical and mechanical dynamic equations based on the above discussions should be solved simultaneously for CSCIM plant:

$$pI_{total} = A_{total}\,I_{total} + B_{total}\,V_{total} \quad (19)$$

Where,

$$I_{total} = [I_1 \quad I_2 \ldots I_j \ldots I_n]^T \quad (20a)$$

$$V_{total} = [V_1 \quad V_2 \ldots V_j \ldots V_n]^T \quad (20b)$$

$$A_{total} = \text{diag}\,[A_1 \quad A_2 \ldots A_j \ldots A_n]^T \quad (21a)$$

$$B_{total} = \text{diag}\,[B_1 \quad B_2 \ldots B_j \ldots B_n]^T \quad (21b)$$

And:

$$p\omega_{total} = T_{total} - D_{total}\,\omega_{total} + K_{total}\,\theta_{total} \quad (22)$$

Where,

$$\omega_{total} = [\omega_{r1} \quad \omega_{r2} \quad \ldots \quad \omega_{rj} \quad \ldots \quad \omega_{rn} \quad \omega_L]^T \quad (23)$$

$$T_{total} = \left[\frac{T_{el}}{J_1} \quad \frac{T_{e2}}{J_2} \quad \cdots \quad \frac{T_{ej}}{J_j} \quad \cdots \quad \frac{T_{en}}{j_n} \quad \frac{T_L}{J_{sh}+J_L}\right]^T \quad (24)$$

$$D_{total} = \text{diag}\left[\frac{D_{el}}{J_1} \quad \frac{D_2}{J_2} \quad \cdots \quad \frac{D_j}{J_j} \quad \cdots \quad \frac{D_n}{j_n} \quad \frac{D_L}{J_{sh}+J_L}\right]^T \quad (25)$$

$$\theta_{total} = [\theta_1 \quad \theta_2 \quad \ldots \quad \theta_j \quad \ldots \quad \theta_n \quad \theta_L]^T \quad (26)$$

$$K_{total} = \begin{bmatrix} -\frac{k_{sh,1}}{J_1} & \frac{k_{sh,1}}{J_1} & 0 & 0 & \cdots 0 \\ \frac{k_{sh,2}}{J_2} & -\frac{(k_{sh,2}+k_{sh,1})}{J_2} & \frac{k_{sh,2}}{J_2} & 0 & \cdots 0 \\ \vdots & \vdots & \vdots & \vdots & \vdots \\ 0 & 0 & \cdots & \frac{k_{sh,n}}{J_{sh}+J_L} & -\frac{k_{sh,n}}{J_{sh}+J_L} \end{bmatrix} \quad (27)$$

Finally:

$$p\theta_{total} = \omega_{total} \quad (28)$$

MODELING OF CSCIMS USING MATLAB SPS BLOCKS

Based on above formulation, simulink diagram for electrical and mechanical parts in cascade scheme shown

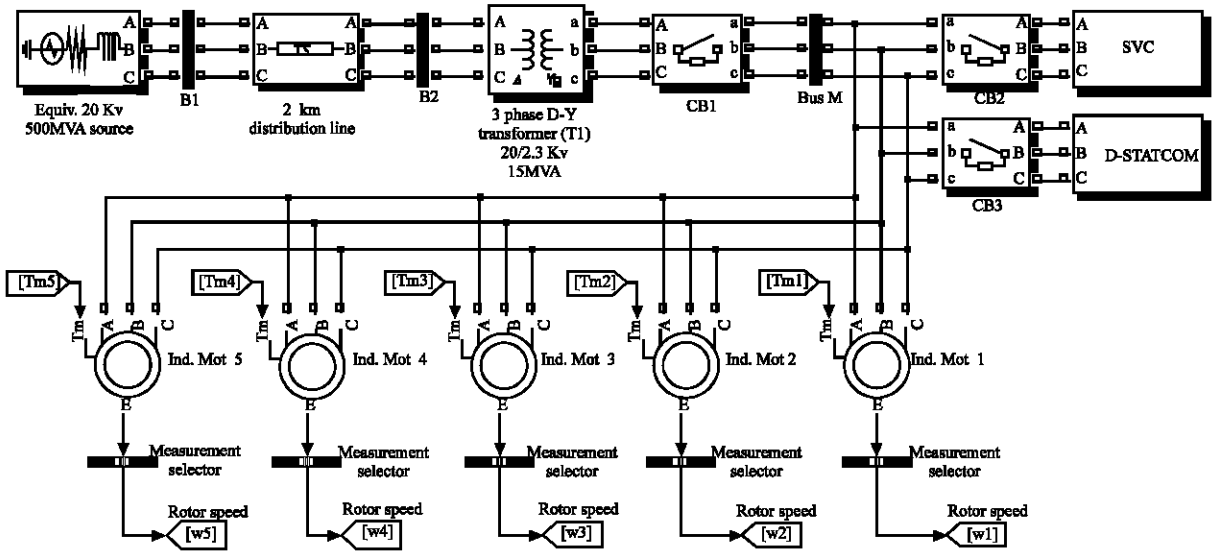

Fig. 2: Simulink diagram for the electrical parts of common shaft cascaded induction motors

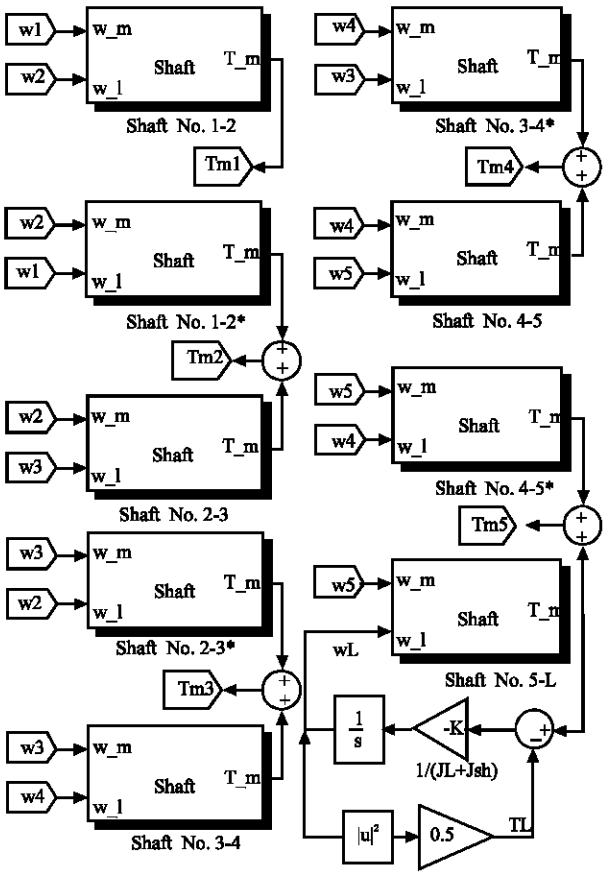

Fig. 3: Simulink diagram for the mechanical parts of common shaft cascaded induction motors

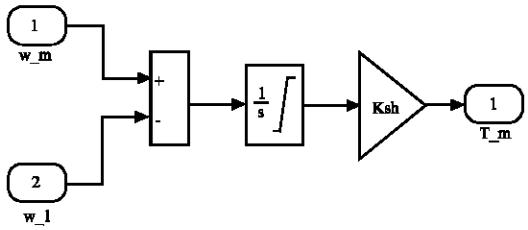

Fig. 4: Simulink diagram for each shaft segment in Fig. 3

in Fig. 1 can be illustrated as Fig. 2 and 3, respectively. In present study it is assumed that there are 5 similar cascade motors and mechanical load is coupled to the fifth motor. The detailed representation of SVC and D-STATCOM in simulink environment will be presented in next sections. Figure 4 also shows each shaft segment in simulink environment for clarification of associated blocks in Fig. 3. The related data for cascade scheme are given in Appendix.

APPENDIX

A. Data for each motor:
2250 hp, 2.3 kV, 60 Hz, P = 4,
R_s = 0.09 Ω, R_r = 0.09 Ω,
L_{ls} = 1.52 mH, L_{lr} = 1.52 mH, L_m = 34.6 mH,
J = 123 kg m^{-2}, D = 0.

B. Shaft Data:
$K_{sh,1} = k_{sh,2} = k_{sh,3} = k_{sh,4}$ = 200 000, $k_{sh,5}$ = 100 000.
J_{sh} = 55 kg m^{-2}.

C. Mechanical load data:
$T_L = 0.5\omega_L^2$ N.m, J_L = 5 kg m^{-2}, D_L = 0.

D. Two km Distribution line and transformer data:
60 Hz, 3phase, transposed line with following positive, negative and zero sequence data:
R1 = R2 = 0.1153 ohms km^{-1}, R0 = 0.3963 ohms km^{-1},
L1 = L2 = 1.048e-3 H km^{-1}, L0 = 2.730e-3 H km^{-1},
C1 = C2 = 11.33e-9 F km^{-1}, C0 = 5.338e-9 F km^{-1},
All transformers assumed to be ideal.

E. D-Statcom Data:

DC Link Voltage	:	Vdc = 10kV;
AC Voltage Regulator	:	Kp = 1, Ki = 10;
DC Voltage Regulator	:	Kp = 1, Ki = 10;
Current Regulator Data	:	Kp = 1, Ki = 10, Kf = 0.22.

D-STATCOM MODELING USING SPS BLOCKS

As mentioned previously, a D-STATCOM is a power electronic system which mainly is equipped with a complex control system (Giroux *et al*., 2001). In this study, it is assumed that a ±3 MVar D-STATCOM is connected to sample system via coupling transformer T3 and associated circuit breaker (CB3). Figure 5 depicts a simulink diagram which represents the D-STATCOM. The primary side of coupling transformer T3 is fed by a voltage source pulse width modulation (PWM) inverter consisting of two isolated gate bipolar transistor (IGBT) bridges. A low pass filter bank is also employed at the inverter output to absorb harmonics. A 1000 μF capacitor is used as dc voltage source for the inverters. In the proposed scheme, it is assumed that a PWM pulse generator with a carrier frequency of 1.76 kHz is used to control both IGBT bridges. The employed modulation scheme is sinusoidal type. The control system block for D-STATCOM shown in Fig. 5 is clarified by diagram shown in Fig. 6. This figure shows that the control system consists of several subsystems such as: Three-phase Phase Lock Loop (PLL), measurement system, current regulator, dc and ac voltage regulators. The function of above subsystems is extensively described in Giroux *et al.* (2001) and Sim Power Systems (2006).

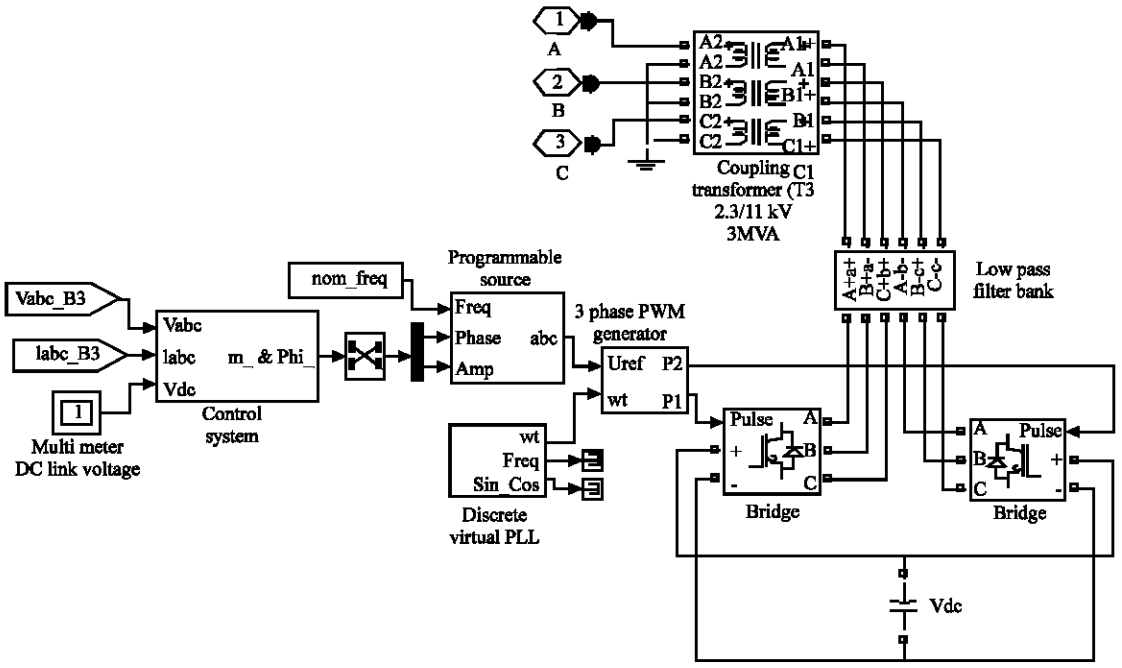

Fig. 5: Simulink diagram for D-STATCOM

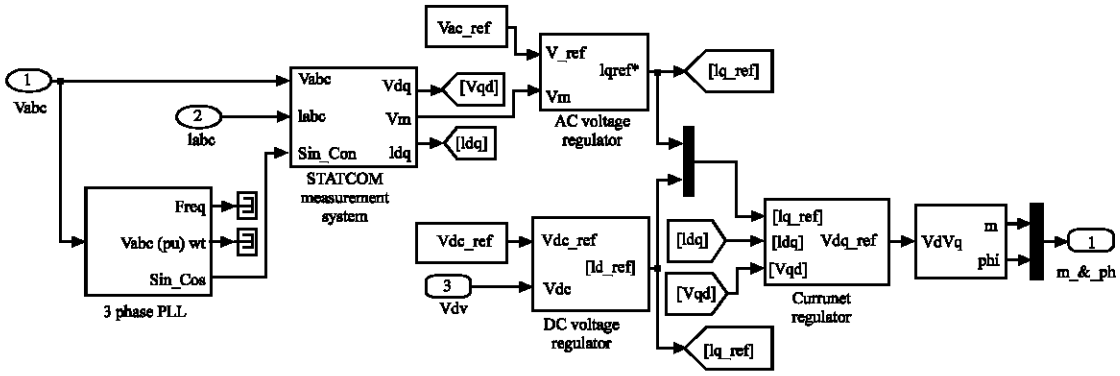

Fig. 6: Simulink diagram for D-STATCOM control system

SVC MODELING USING SPS BLOCKS

As mentioned previously, SVC is usually composed of Thyristor Controlled Reactor (TCR) and Thyristor Switched Capacitor (TSC) associated with a control system to regulate its terminal voltage. In this study, we consider a 4 MVar device including 3 TSCs (3×1 MVar) and one TCR (1×1 MVar) which is connected to sample system through coupling transformer (T2) and associated circuit breaker (CB2). The SVC is connected to primary side of 11/2.3kV, 4 MVA 3 phase coupling transformer (T2). Each 3-phase bank in TCR and TSC scheme is connected in delta therefore during normal balanced operation triple harmonic components (3rd, 9th...) would be trapped providing reduction in harmonic injection into the power system. Figure 7 shows the simulink diagram for employed SVC. Using proposed configuration, TSCs switching provides a discrete variation of reactive power in primary side of transformer (T2) from zero to 3 capacitive MVar with 1 MVar steps. However the phase control of TCR provides a continuous variation of reactive power from zero to 1 inductive MVar. Figure 8 shows a simulink diagram representing the SVC controller. This figure shows that the controller consists of several subsystems such as: Measurement system, voltage regulator, Distribution unit, Firing unit. A detailed description of the subsystems is given in Sim Power Systems (2006). The SVC controller monitors the voltage

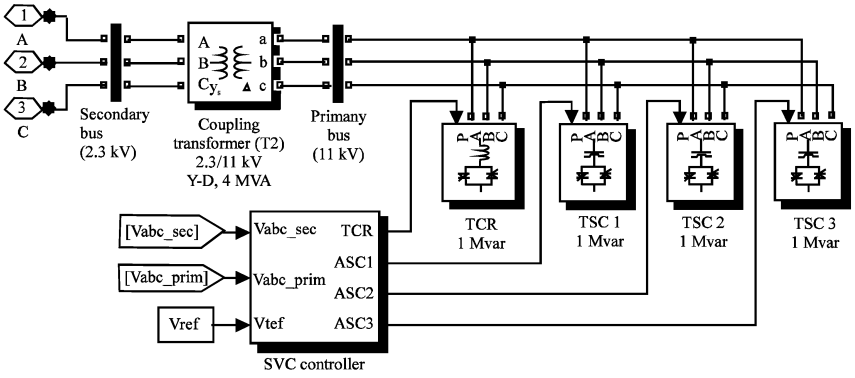

Fig. 7: Simulink diagram for SVC connected to main bus (bus M)

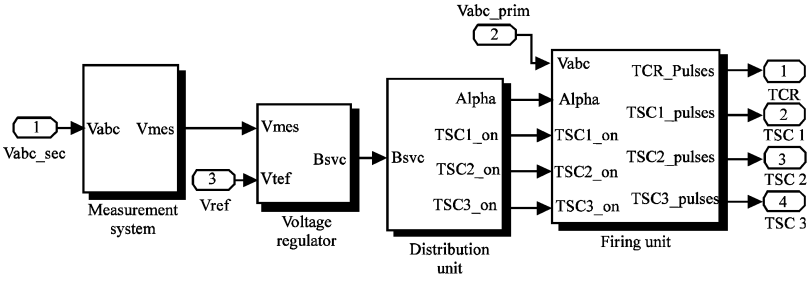

Fig. 8: Simulink diagram for SVC controller

at secondary side of transformer (T2) and provides appropriate pulses for 24 thyristors (6 thyristors per 3-phase TCR and TSC bank) in order to obtain the appropriate susceptance required by voltage regulator.

SIMULATION RESULTS

The simulation results presented in this study is related to transient and dynamic performance of five similar 3 phase CSCIMs in presence of SVC (i.e. CB2 is closed) or D-STATCOM (i.e. CB3 is closed). The system data are given in Appendix. All results presented for different cases belong to behaviour of the fifth motor (i.e. the nearest motor to mechanical load).

Starting: In this case, it is assumed that all CSCIMs are started at t = 0 by closing relevant circuit breaker (CB1) in no load condition (i.e. no mechanical load acting against the common shaft). Figure 9-12 illustrate the speed, torque, terminal voltage and stator current of fifth motor during starting period. It can be seen that the D-STATCOM makes the starting process faster (i.e. according to the starting time in Fig. 9), easier (i.e. according to the starting torque in Fig. 10) and superior in quality (i.e. according to the terminal voltage and the motor starting current in Fig. 11 and 12) with respect to SVC.

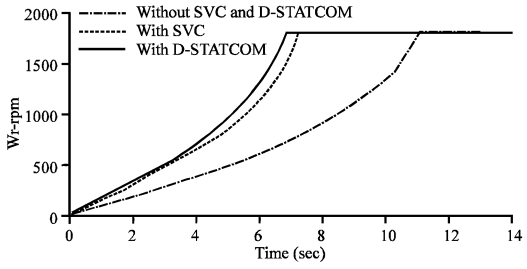

Fig. 9: Speed of fifth motor for case 1

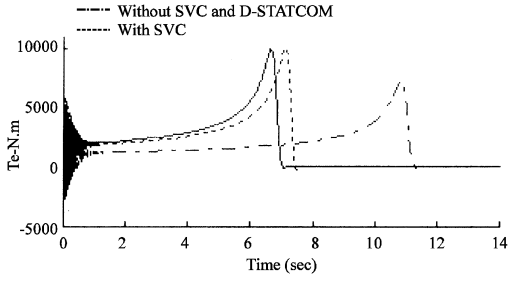

Fig. 10: Torque-time characteristic of 5th motor for case 1

Supply voltage sag and swell: In this case it is assumed that after loading process a 10% supply voltage sag is occurred at t = 20 sec at the sending end of 20-kV distribution line and is cleared at t = 21 sec. It is also

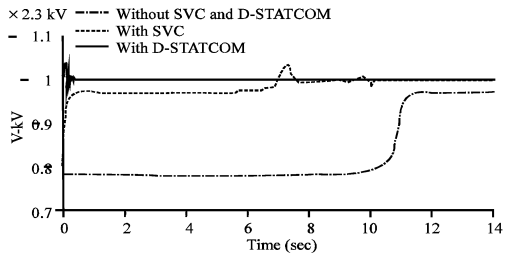

Fig. 11: Main bus phase to phase rms voltage for case 1

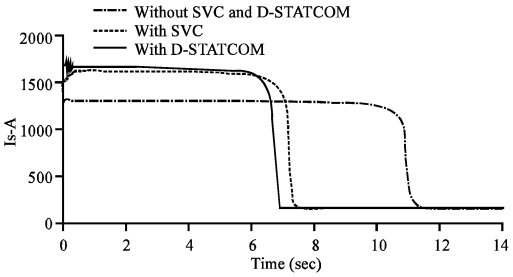

Fig. 12: Stator rms phase current of fifth motor for case 1

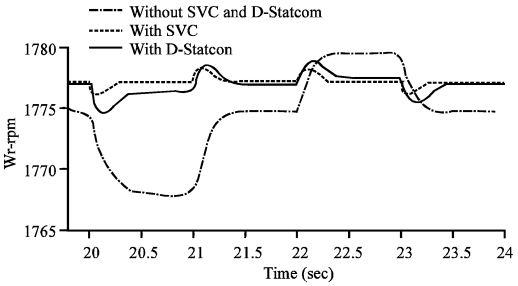

Fig. 13: Speed of fifth motor for case 2

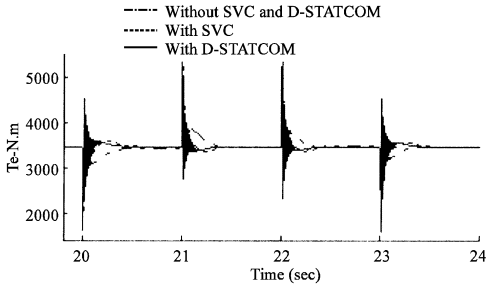

Fig. 14: Torque-time characteristic of fifth motor for case 2

assumed that a 10% voltage swell is occurred at t = 22 sec at the sending end of 20-kV distribution line and is cleared at t = 23 sec. Figure 13-16 show the speed, torque, terminal voltage and stator current of fifth induction motor related to this case. It can be seen that the D-STATCOM has a superior performance over SVC in order to regulate motor speed (Fig. 13), motor torque (Fig. 14),

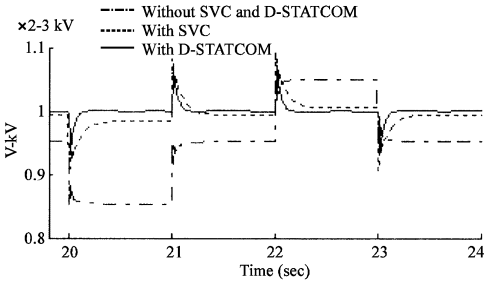

Fig. 15: Main bus phase to phase rms voltage for case 2

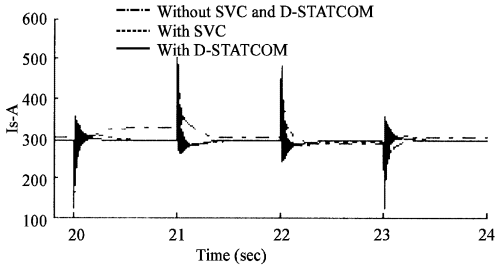

Fig. 16: Stator rms phase current of fifth motor for case 2

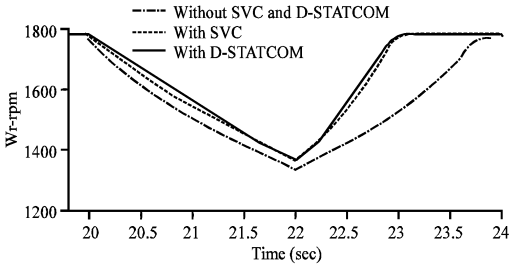

Fig. 17: Speed of fifth motor for case 3

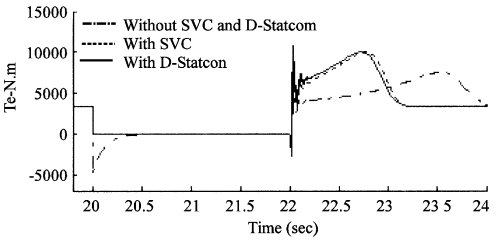

Fig. 18: Torque-time characteristic of fifth motor for case 3

terminal voltage (Fig. 15) and motor current (Fig. 16) during the sag and swell events.

Supply disconnection and reconnection: In this case it is assumed that after loading process, the supply is disconnected at t = 20 sec (i.e. CB1 is opened) and reconnected at t = 22 sec (i.e. CB1 is closed). Figure 17-20 show the speed, torque, terminal voltage and stator current of 5th induction motor related to supply

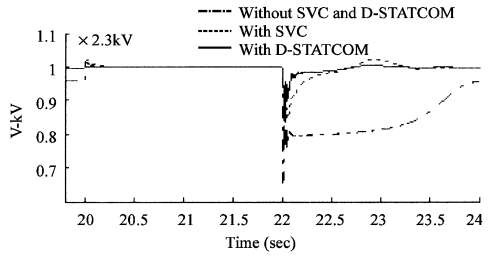

Fig. 19: Main bus phase to phase rms voltage for case 3

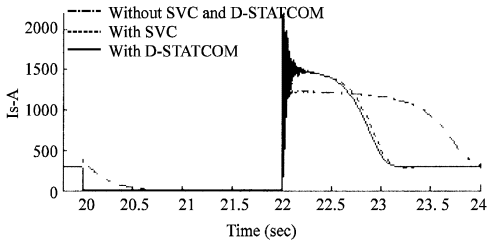

Fig. 20: Stator rms phase current of fifth motor for case 3

disconnection and reconnection. It can be seen that the D-STATCOM has a superior performance over SVC in order to regulate motor speed (Fig. 17), motor torque (Fig. 18), terminal voltage (Fig. 19) and motor current (i.e. Fig. 20) during supply reconnection event. It can also be seen that the SVC and D-STATCOM has approximately a same performance during supply disconnection event.

CONCLUSION

This study presents the comparative studies in order to evaluate the effects of SVC and D-STATCOM on dynamic and transient performance of CSCIMs. To achieve this aim, 3 case studies are presented and detailed simulation is performed using well known MATLAB/Simulink software. The results show that the D-STATCOM has a superior performance over SVC in order to enhance the dynamic performance of CSCIMs. In the present paper the efforts have been made to regulate the motors terminal voltage by SVC and D-STATCOM in order to enhance the dynamic responses. Regulation of more than one index at the same time (i.e. load power factor and load terminal voltage) using other FACTS device such as unified power quality conditioner (UPQC) is a subject of authors' present research.

Nomenclature:

D : Viscous friction coefficient.
I : Current.
J : Moment of inertia.
K : Stiffness factor.
L : Inductance.
M : Mutual inductance between stator and rotor windings.
p : = d/dt.
P : Number of poles.
R : Resistance.
T_e, T_L : Motor and load torques.
T_f : Friction torque.
T_m : Shaft stiffness torque.

Greek letters

α : Supply phase angle (= 0).
θ : Rotor angular position.
ω_L : Load speed.
ω_r : Rotor speed.
t : Time.

Subscripts

d, q : Direct- and quadrature-axis quantities
a, b, c : Phase quantities.
j : Motor number.
l : Leakage quantities.
r, s : Rotor and stator quantities.
sh : Shaft quantities.
0 : Zero sequence.

REFERENCES

Abdel-Rahman, M.H., F.M.H. Yousef and A.A. Saber, 2006. New Static Var Compensator Control Strategie and coordination with under-load tap changer. IEEE Trans. Power Del., 21: 1630-1635.

Abedi, M., M.R. Maher and R. Madahi, 1995. Evaluation of the transient performance of cascade induction motors, Elsevier. Elec. Power Syst. Res., 32: 133-140.

Abedi, M., S.A. Taher, A.K. Sedigh and H. Seifi, 1998. Controller design using μ-synthesis for static var compensator to enhance the voltage profile for remote induction motor loads. Elec. Power Syst. Res., 46: 35-43.

Adkins, B. and R.G. Harley, 1975. The General Theory of Alternating Current Machines. Chapman and Hall, London.

Boldea, I. and S.A. Naser, 1986. Electrical Machine Dynamics. Macmillan, New York.

Chang, C.S. and Yu Qizhi, 1999. Fuzzy bang-bang control of static VAR compensators for damping system-wide low-frequency oscillations, Elsevier. Elec. Power Syst. Res., 49: 45-54.

Eldery, M.A., E.F. El-saodany and M.M.A. Saloma, 2007. DSTATCOM Effects on the Adjustable Speed Drive Stability Boundaries. IEEE Trans. Power Del., 22 (2): 1202-1209.

Freitas, W., A. Morelato, Xu Wilsun and F. Sato, 2005. Impact of AC Generators and DStatcom devices on the transient performance of distribution systems. IEEE. Trans. Power Del., 20 (2): 1493-1501.

Giroux, P., G. Sybille and H. Le-Huy, 2001. Modeling and Simulation of a Distribution STATCOM using Simulink's Power System Blockset, In IECON'01: 27th Annu. Conf. IEEE Ind. Electron. Soc., 2: 990-994.

Hancook, N.N., 1974. Matrix Analysis of Electrical Machinery. Pergamon, Oxford.

Jing Zhang, J.Y. Wen, S.J. Chang, Jia and Ma, 2007. A Novel SVC Allocation Method for Power System Stability Enhancement by Normal Forms of Diffeomorphism. IEEE Trans. Power Syst., 22: 1819-1825.

Krause, P.C., 1965. Simulation of symmetrical induction machinery. IEEE Trans. Power Applied Syst., 84: 1038-1053.

Krause, P.C., 1986. Analysis of Electric Machinery. McGraw-Hill, New York.

Lin, W.C., C.E. Lin, C.L. Huang, S.L. Chen and Y.T Wang, 1986. Prediction of the transient performance of induction machines. Elec. Power Syst. Res., 10: 241-246.

Nath, G. and G.J. Berg, 1981. Transient analysis of 3 phase SCR controlled induction motors. IEEE Trans. Ind. Applied, 17: 133-142.

Ogata, K., 1970. Modern Control Engineering, Prentice-Hall, Englewood Cliffs, NJ.

Rastegar, H., M. Abedi, M.B. Menhaj and S.H. Fathi, 1999. Fuzzy Logic based static Var compensators for enhancing the performance of synchronous and asynchronous motor loads. Elec. Power Syst. Res., 50: 191-204.

Sarka, A.K. and G.J. Berg, 1970. Digital simulation of 3 phase induction motors. IEEE Trans. Power Applied Syst., 89: 1031-1037.

Sensarma, P.S., K.R. Padiyar and V. Ramanarayanan, 2002. Analytical Performance of a Distribution STATCOM for Compensating Voltage Fluctuations. IEEE Trans. Power Del., 16: 259-264.

Sim Power Systems, 2006. For Use with Simulink, User's Guide. The MathWorks, Inc.

Smith, I.R. and S. Sriharam, 1967. Induction motor reswitching transients. Proc. Inst. Electr. Eng., 114: 503-509.